Polarization controlled UV writing of bragg gratings

Jensen, Jesper Bo Damm; Plougmann, Nikolai; Deyerl, Hans-Jürgen; Kristensen, Martin

Published in:
Optical Fiber Communication Conference and Exhibit, 2002. OFC 2002

Link to article, DOI:
10.1109/OFC.2002.1036240

Publication date:
2002

Document Version
Publisher's PDF, also known as Version of record

that the MPS technique is applicable not only to simple sampled FBG's, but also to various kinds of complex (superstructure) FBG's, such as apodized, sinc-, and chirped sampled FBG's.

3. Apodized-sampled FBG with MPS

Apodzation of sampled FBG's can suppress the unwanted sidelobes. We confirmed that the MPS technique is applicable to apodized-sampled FBG's both in a simulation (Fig. 2) and an experiment (Fig. 3). In the experiment, first we fabricated a conventional apodized-sampled FBG (Fig. 3(a)). Then we introduced phase shifts (m = 2: $\phi = 0, \pi, 0, \pi, \ldots$) as a post-process. Irradiation of UV light was stopped when the reflection spectrum reached optimum. We could successfully halve the channel spacing, although the side-mode suppression becomes worse than the simulation (Fig 3. (b)), which may be due to nonideal phase shifts.

4. Sinc-sampled FBG with MPS

Sinc-sampled FBG has sinc-shaped modulation of the refractive index in order to suppress sidelobes and to equalize the each channel bandwidth. We also applied the MPS technique to sinc-sampled FBG's. Fig. 4(a) shows the reflection spectrum of 3-channel sinc-sampled FBG having the total length of 100 mm. When the phase shifts (m = 4) are introduced, the channel spacing is reduced to 1/4 in simulation (Fig. 4(b)). To increase the number of channels in the conventional sinc-sampled FBG's, more complex modulation in the refractive index is needed. In contrast, the MPS technique can increase the number of channels without complex modulation, at the cost of enhanced sidelobes.

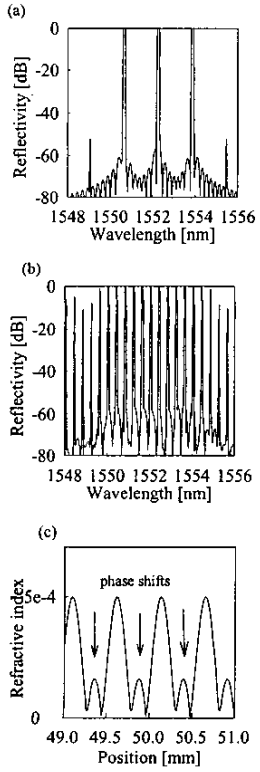

TuQ3 Fig. 4. Sinc-sampled FBG. (a) without MPS, (b) with MPS (m = 4). (C) Refractive index distribution.

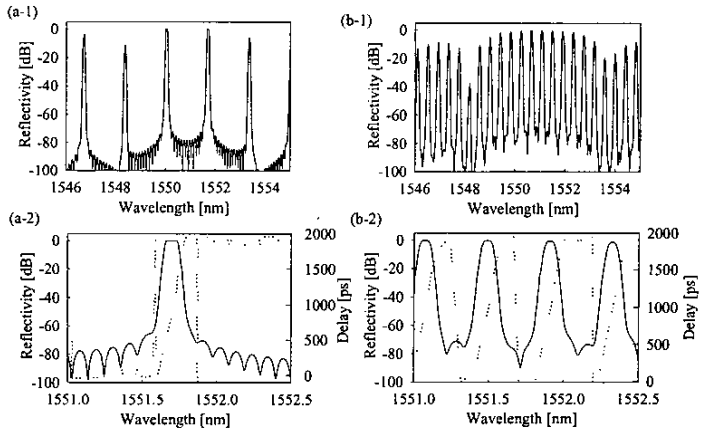

TuQ3 Fig. 5. Chirped-sampled FBG. (a) without MPS. (b) without MPS.

5. Chirped-sampled FBG with MPS

Chirped-sampled FBG's whose grating period changes along the fiber can be used for multi-channel dispersion compensator. We also applied the MPS technique to chirped-sampled FBG's. Calculated reflection spectra and delay characteristics of chirped-sampled FBG with and without MPS are shown in Fig. 5. Chirp rate is assumed to be 0.01 nm/cm, amplitude of refractive index modulation 10^{-4}, total length 200 mm and FBG period 0.5 mm. We found that the MPS technique can densify the channel spacing with keeping delay characteristics.

6. Conclusion

We showed and demonstrated that the MPS technique is applicable to not only simple sampled FBG's, but also various kinds of complex (superstructure) FBG's, such as apodized, sinc-, and chirped sampled FBG's. We believe that MPS technique is very useful to many kinds of superstructure FBG's.

References

1. M. Ibsen *et al., IEEE Photon. Technol. Lett.*, vol. 10, no. 6, pp. 842–844, 1998.
2. M. Ibsen *et al., Electron. Lett.*, vol. 10, pp. 84–86, 1988.
3. Xiang-fei Chen *et al., Photon. Technol. Lett.*, vol. 12, no. 11, 2000.
4. W. H. Loh *et al., Opt. Lett.*, vol. 24, no. 21, pp. 1457–59, 1999.
5. F. Ouellette *et al., Electron. Lett.*, vol. 31, no. 11, pp. 899–901, 1995.
6. Y. Nasu and S. Yamashita, *IOOC/OECC 2001*, no. PDP 1.06, 2001.

TuQ4 **2:45 pm**

Polarization controlled UV writing of Bragg gratings

Jesper Bo Jensen, Nikolai Plougmann, Hans-Jürgen Deyerl and Martin Kristensen, *COM, Technical University of Denmark, Building 345v, DK-2800 Kgs. Lyngby, Denmark, Email: jbj@com.dtu.dk*

1. Introduction

As the demand for bandwidth in optical communication systems continues to grow much effort is put into a more efficient use of the available wavelength span through the wavelength division multiplexing (WDM) technique. While the next generation electronic components will be able to handle 40 Gbit/s signals, the development in WDM systems is pushing the ITU channel spacing down to 50 GHz and in time 25 GHz. As the channel spacing decreases, the spectral properties of the individual components such as Bragg gratings becomes crucial. Bragg gratings working as channel selective components must have high bandwidth utilization and low out-of-band reflection in order to avoid cross-talk induced problems. In order to avoid an increasing bit-error rate when cascading several gratings the variation in the signal reflection and dispersion in the stop band must be small. The transmission dip must be 30 dB and the side lobe suppression in the reflection spectrum must exceed 30 dB. Gratings with simple apodization profiles, such as Gaussian and Blackmann apodizations are not able to satisfy all these demands. The Sinc grating on the other hand has almost a square filter function with a flat stop band and little reflection outside this. Problems with dispersion can be reduced to acceptable levels by assymmetric modification of the Sinc profile.[1] Sinc gratings require several phase shifts, which is not possible to induce with the dual-scan method.[2] A frequently used method to write Bragg gratings with multiple phase shifts is the dithering method[3] where fiber and/or phase mask are moved during the exposure. This method requires interferometric control of the relative position of the fiber and phase mask and is hence very sensitive to vibrations in the setup. We present a method, which is based on a spatial separation of the s- and p-polarizations of the UV beam.[4] Using this method we have been able to write 80 dB strong gratings with good agreement between simulations and written gratings.

2. Principle

A schematic presentation of the principle of the polarization control method is seen in Figure 1. A polarization beam splitter moves along the phase mask together with the UV beam. Both fiber and phase mask are stationary during the exposure making the polarization control method less sensitive to vibrations than the dithering method. The polarization beam splitter introduces an angle between the propagation vectors of the s- and p-polarizations of the UV beam. In the fiber

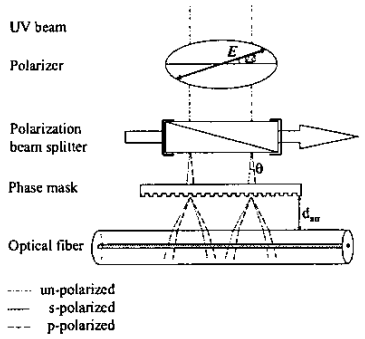

TuQ4 Fig. 1. Schematic presentation of the polarization control method. Two spatially separated Bragg gratings are generated in the fiber core by the diverging s- and p-polarized fractions of the UV beam. The ratio of UV intensity in the polarizations and hence the relative strength of these gratings is controlled by a polarizer mounted on a computer controlled rotation stage.

core the diverging beams write two spatially separated Bragg gratings. The phase shift between these gratings depends on the optical distance from the phase mask and the divergence angle θ of the polarization beam splitter. By adjusting the distance between phase mask and fiber, d_{air}, we can hence define arbitrarily large phase shifts in the overall Bragg grating by shifting the UV intensity from one polarization to the other. A discrete phase shift of π is obtained in the overall Bragg grating when d_{air} is given by

$$4\theta\,(d_{air} + r_{fiber}/n_{clad}) = \Lambda_{mask} \qquad (1)$$

where r_{fiber} is the fiber radius, n_{clad} is the refractive index of the fiber cladding at 248 nm and Λ_{mask} is the phase mask period. The divergence angle is assumed to be small, so that the assumption $\sin\theta \approx \tan\theta \approx \theta$ is justified. The beam splitter used in our setup is a Wollaston prism with a divergence angle of 0.14 degrees. With a fiber diameter of 125 μm, d_{air} is in the order of 68 μm for a Bragg grating with a center wavelength around 1550 nm. Adjustment of this distance must be very accurate in order to obtain high quality gratings. The ratio of UV intensity in the two polarizations is controlled by a polarizer mounted on a computer controlled rotation stage. With α denoting the angle of the polarizer relative to the s-polarization, the fluences in the two polarizations are $F_s = F\cos^2\alpha$ and $F_p = F\sin^2\alpha$ respectively, where F is the total fluence of the beam. Due to the discrete π phase shift between the two polarizations the UV induced refractive index modulation strength $\Delta n(z)$ in the resulting Bragg grating is described by

$$\Delta n(z) = \eta F + \eta F\cos(2\alpha)\cos\left(\frac{2\pi z}{\Lambda_B} + \phi_0\right) \qquad (2)$$

where z is the position along the fiber, ϕ_0 is a constant and η describes the photosensitivity of the fiber. Equation 2 shows that the change in the effective refractive index, ηF, is constant along the fiber, while the modulation amplitude scales with $\cos(2\alpha)$. Thus by rotating the polarizer we are able to change the modulation strength while maintaining a constant effective refractive index. Maximum modulation strength is obtained when the polarizer angle is either 0° or 90°, that is when only one polarization is present, while zero modulation is achieved when α = 45° and the UV intensity in the s-polarization equals that in the p-polarization. The period of the resulting Bragg grating is $\Lambda_B = n_{eff}\Lambda_{mask}$, where n_{eff} is the effective refractive index after the exposure. The normalized fluence profiles for the two polarizations and the resulting apodization profile for writing a Sinc grating is seen in Figure 2(a), while Figure 2(b) shows the corresponding polarizer angle profile. The Sinc grating had an additional Gaussian apodization to avoid problems due to the finite length of the grating. This reduces the steepness of the sides of the reflection peak, but is necessary to obtain strong side lobe suppression as may easily be seen from simulations. As indicated in Figure 2 we obtain a π phase shift in the grating whenever the polarizer angle crosses over the α = 45° line, which is marked with a dotted line in the figure.

3. Experimental results

The UV source is a pulsed KrF Excimer laser, which gives a slightly polarized beam. A tilted quartz window placed at the exit of the laser equalizes the UV intensity in the two polarizations. The polarization control method was used to write Sinc gratings in a Highly Non-Linear Fiber (HNLF) and the non zero dispersion TrueWave® fiber both supplied by Lucent Technologies Denmark. All fibers were sensitized by 14 days deuterium loading at room temperature at 120 bar. In our writing setup the fiber photosensitivity is assumed to be independent of accumulated fluence and polarization of the UV beam. The polarization dependence was tested on a non-sensitized HNLF-fiber and showed only a negligible dependence. We furthermore expect this to be the case for both sensitized HNLF- and TrueWave®-fiber. While the induced change in refractive index versus fluence is independent of the accumulated fluence for the TrueWave®-fiber a pre-exposure of 30–60 J/cm^2 was required to raise the HNLF-fiber into a linear regime. With the additional Gaussian apodization we were able to obtain Sinc-gratings with a side lobe suppression of 27 dB for weak gratings, while the suppression is somewhat smaller for the stronger gratings.

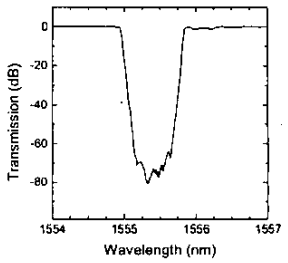

TuQ4 Fig. 3. A 23 mm Gaussian grating written in a deuterium loaded HNLF fiber using only a single exposure.

Figure 2 shows measured and simulated reflection and transmission spectra for a 23 mm long Sinc grating written in a HNLF-fiber. Weaker gratings with a better side lobe suppression than that obtained in this grating were easily written as well as gratings with transmission dip of 50 dB. Furthermore we have written a 23 mm long grating with a pure Gaussian apodization showing a transmission dip of 80 dB as seen in Figure 3.

4. Conclusion

In conclusion the polarization control method is superior to any double scan method since it allows much more flexible apodization and inclusion of phase shifts, and since only one exposure is required. In many cases the method performs just as well as the most sophisticated phase mask jitter methods, while still remaining very simple and robust.

References

1. M. Ibsen, P. Petropoulos, M.N. Zervas and R. Feced, "Dispersion-free fibre Bragg gratings," in OSA *Trends in Optics and Photonics (TOPS) Vol. 54, Optical Fiber Communication Conference,* Technical Digest, Confer-

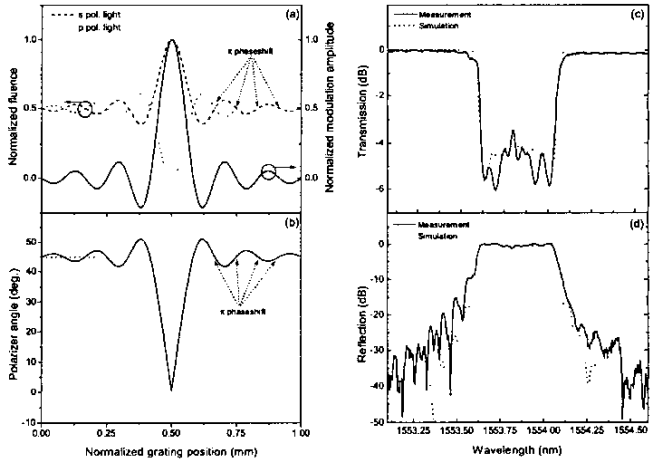

TuQ4 Fig. 2. (a) Normalized fluence profiles for the s- and p-polarizations and modulation amplitude and (b) the corresponding polarizer angle for a Sinc grating. The dotted line at α = 45° marks the cross over between segments of the grating with different phase. Transmission (c) and reflection (d) spectra for a 23 mm long Sinc-grating written in deuterium loaded HNLF fiber.

ence Edition (Optical Society of America, Washington DC, 2001), paper MC1.
2. R. Kashyap, A. Swanton, and D.J. Armes, "Simple method for apodising chirped and unchirped fibre Bragg gratings," Electron. Lett. 32, 1226–1228 (1996).
3. P. Varming, J.B. Jensen, N. Plougmann, M. Kristensen and J. Hübner, "New and simple method for fabrication of advanced UV written Bragg gratings," in *Bragg gratings, Photosensitivity, and Poling in Glass Waveguides*, OSA Technical Digest, (Optical Society of America, Washington DC, 2001), paper BW A5-1.
4. M.J. Cole, W.H. Loh, R.I. Laming, M.N. Zervas, and S. Barcelos, "Moving fibre/phase mask-scanning beam technique for enhanced flexibility in producing fibre gratings with uniform phase mask," Electron. Lett. 31, 1488–1490 (1995).

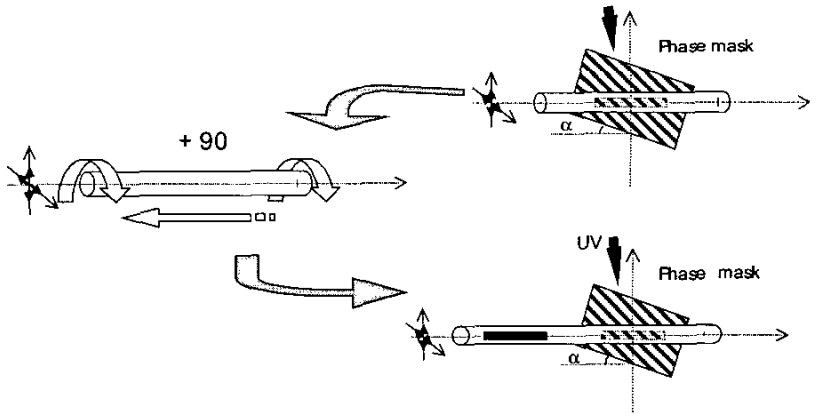

TuQ5 Fig. 1. Schematic process for manufacturing slanted Bragg gratings with ultra-low Polarization Dependent Loss (PDL).

TuQ5 **3:00 pm**

Slanted Bragg grating with ultra-low polarization dependant loss

H. Labidi, C. Debarros, R. Letteron and I. Riant, *ALCATEL CIT Route de Nozay 91460 Marcoussis, France, Email: hedi.labidi@ms.alcatel.fr*

1. Introduction

It has been shown that the slanted Bragg grating (SBG) is a highly attractive candidate for equalizing the gain spectrum of erbium doped fiber amplifiers (EDFAs).[1] This is a standard Bragg grating tilted during photo-inscription with an angle between the grating fringes and the normal of the fiber axis. This makes the grating couple most of the guided mode into radiation modes or cladding modes in a counter-propagating direction. The filter shape is therefore given by the envelope of couplings into the different cladding modes. The SBG exhibits the absence of back-reflection at filtering wavelengths of long period grating and the properties of the grating are as robust as those of standard short period grating in terms of temperature sensitivity and strain.[2]

SBGs exhibit generally low polarization sensitivity, typically around 0.1 dB for angles around 4°–5° in the fiber. When the angle is increased or when certain types of fibers are use[3] SBG may behave a little differently and present higher values of Polarization Dependent Loss (PDL), above 0.2 dB, and this is intolerable for use as gain equalizers for long transmission links. Here is presented a simple and low cost solution to reduce this PDL to very low value without modifying the spectral shape of the filter.

2. Experiments

Let's consider the slanted Bragg grating to be a mirror and the electric field of the fundamental guided mode LP_{01} to be split up into its two planes of polarization, parallel and perpendicular. The two polarizations are reflected differently. A second mirror placed at 90° reflects the opposite polarizations, the perpendicular one instead of the parallel one and vice versa. The combination of the two mirrors makes the reflection independent to the polarization state of the incident light.

The solution we proposed in then based on the photo-inscription of two slanted Bragg gratings at 90° from each other about fiber axis. We propose a two step writing. We first photo-imprint one slanted grating, then rotate the fiber around its axis, by 90°, translate the fiber (It is possible also not to translate the fiber), as described in Fig. 1, and write a second grating. The usual time of inscription of a complete grating is divided by two and distributed between the two rotated half gratings.

Two slanted Bragg gratings called SBG1 and SBG2 are photo-written in a fiber along Z axis, inclined at an angle α with respect to a normal plane N to Z axis. Two writing planes called P1 and P2 are defined forming an angle α with normal plane N and an angle θ about Z axis between them. θ called the rotation angle is between 60° and 120° (Fig. 2).

3. Results and discussion

An example is shown below on Fig. 3 for SBGs inclined at approximately 7.2° in the fiber for a contrast of –3.5 dB. The triangles represent the PDL of a slanted grating photo-imprinted without any rotation. This grating exhibits a PDL of nearly 0.25 dB. The squares represent the PDL of a slanted grating realized with the two steps previously described. The PDL has been decreased to 0.03 dB. The experimental demonstration had been done in several types of fiber.

The fact that the two gratings are separated along Z axis proves that it is not due to photo-induced birefringence reduction because of more symmetric UV irradiation[4] as it was early thought when first experiments has been done writing the gratings at the same place.

In order to conserve the spectral shape the two gratings must be identical with the same period, the same angle, the same length, . . .

4. Conclusion

An efficient method has been presented to fabricate slanted Bragg grating based filters with ultra low polarization dependent loss.

References

1. I. Riant et al., Tech. Digest of OFC'99, THj-147/149, 1999.
2. C. De Barros et al, "Tapered slanted Bragg grating for low insertion loss", OSA technical Digest: Conference on Bragg Gratings photosensitivity and poling in glass waveguides, Stresa, Italy, (paper JW1), BGPP '01.
3. I. Riant et al., Tech. Digest of Suboptics-01, Japan, P.4.3.10, pp. 551–553, 2001.
4. Ashish M. Vengsarkar et al., "Birefringence reduction in side-written photoinduced fiber devices by a dual-exposure method" Optics Letters, vol. 19, n° 16, pp. 1260–1262, August 15, 1994.

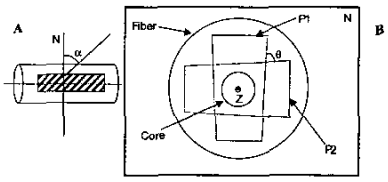

TuQ5 Fig. 2. Schematic side (A) cross-sectional (B) view of one of the slanted Bragg gratings and the two writing planes as defined in the text.

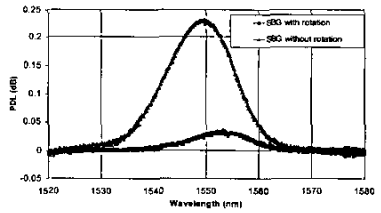

TuQ5 Fig. 3. The PDL spectrum (in dB) as a function of wavelength (in nm).

TuQ6 **3:15 pm**

Novel Laser Fusion Processes of Fabricating Low-Loss S-band WDM Narrowband Coupler Devices Overcome H_2O Resonant Absorption

Xu Liu, Erkin Sidick, Tracy Brewer, Joseph Chon, and Frank Liang, *Wavesplitter Technologies, Inc., 46430 Fremont Blvd., Fremont, CA 94538, Email: Joseph_Chon@WaveSplitter.com*

1. Introduction:

Optical amplifiers have stimulated all-optical signal transmission in long-haul, metro core and metro communication systems without using expensive O/E/O re-generators. The output power of an optical amplifier determines the maximum distance to the next amplifier and the possible number of fan-outs in a broadcasting network. In